Supplementary Information (SI) for ChemComm.
This journal is © The Royal Society of Chemistry 2025

Multi-color luminescent crystals derived from dynamic diastereomers of a perylene-substituted binaphthol derivative

Riko Yano[a] and Suguru Ito*[ab]

[a] *Department of Chemistry and Life Science, Graduate School of Engineering Science, Yokohama National University*
79-5 Tokiwadai, Hodogaya-ku, Yokohama 240-8501, Japan.
*E-mail: suguru-ito@ynu.ac.jp

[b] *PRESTO, Japan Science and Technology Agency (JST),*
4-1-8 Honcho, Kawaguchi, Saitama 332-0012, Japan.

Table of contents

1. General

All air-sensitive experiments were carried out under an argon atmosphere unless otherwise noted. (*S*)-(2,2′-Dimethoxy-[1,1′-binaphthalen]-3-yl)boronic acid and 3-bromoperylene were synthesized according to the literature procedures.[1,2] Silica gel 60 N (spherical, neutral, 63–210 μm) was used for column chromatography. Other reagents and solvents were commercially available and were used as received. IR spectra were recorded on a JASCO FT/IR 6200 spectrometer equipped with an ATR PRO450-S. ^{1}H and ^{13}C NMR spectra were recorded on a JEOL ECA500 spectrometer using tetramethylsilane (^{1}H NMR: 0.00 ppm) or solvent residual signals [^{1}H NMR: DMSO-d_6 (2.50 ppm); ^{13}C NMR: $CDCl_3$ (77.0 ppm)] as an internal standard. The fluorescence images of the crystals were recorded by fluorescence microscopy (BX53, Evident) equipped with a CCD camera (DP23, Evident). Photonic multichannel analyzer (PMA-12 C14631-03, HAMAMATSU) and a LED light (367 nm, EVIDENT U-LGPS, OLYMPUS) were used for the measurements of fluorescence spectra. Fluorescence spectra in solution and UV-vis absorption spectra were measured on a JASCO FP-8300 fluorescence spectrometer. The absolute fluorescence quantum yields were determined using a 100 mm ϕ integrating sphere JASCO ILF-835. The solid-state absorption spectra were obtained by measuring diffuse reflectance spectra using an FPA-810 powder sample cell block, in which a sample diluted in $BaSO_4$ (10 wt%) was loaded. For the measurement of UV-vis absorption spectra in THF and THF/H_2O, an FUV-803 absorbance measurement cell block was used. Fluorescence lifetime measurements were carried out using a HAMAMATSU Quantaurus-Tau fluorescence lifetime spectrometer C16361-01. Electronic circular dichroism (ECD) spectra were recorded on a JASCO J-1100 circular dichroism spectrometer. Samples were dispersed in KBr by grinding, followed by compressing into a transparent pellet. Powder X-ray diffraction (PXRD) measurements were performed on a Rigaku SmartLab system using CuKα radiation. Differential scanning calorimetry (DSC) data were recorded on a Shimadzu DSC-60 plus (heating rate: 2 °C min^{-1}). Melting points were determined on a Stuart melting point apparatus SMP3 and uncorrected. Optical rotation was measured on an Anton Paar MCP 150 polarimeter. High-resolution electrospray ionization mass spectra (HRMS-ESI) were recorded on a Hitachi Nano Frontier LD spectrometer.

2. Synthesis of (*S*)-3-(2,2′-dimethoxy-[1,1′-binaphthalen]-3-yl)perylene

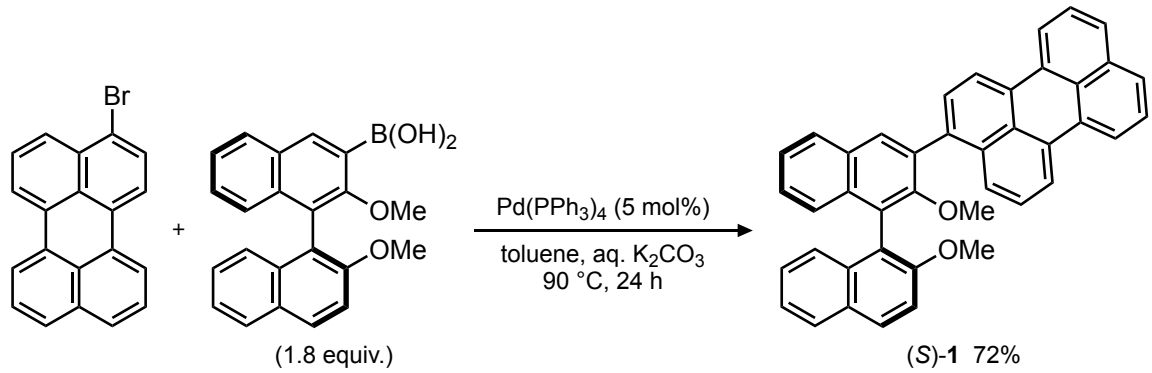

Scheme S1 Synthesis of (*S*)-3-(2,2′-dimethoxy-[1,1′-binaphthalen]-3-yl)perylene [(*S*)-**1**]

To a mixture of (*S*)-(2,2′-dimethoxy-[1,1′-binaphthalen]-3-yl)boronic acid[1] (0.837 g, 2.3 mmol) in toluene (23.4 mL) and 3-bromoperylene[2] (0.428 g, 1.3 mmol) was added 2 M aqueous K_2CO_3 (15.6 mL), and the mixture was degassed under ultrasonic irradiation. To the mixture was added $Pd(PPh_3)_4$ (75.4 mg, 0.065 mmol), and the mixture was further degassed under ultrasonic irradiation. After the mixture was stirred at 90 ºC for 24 h, water and dichloromethane were added to the mixture. The organic layer was separated and the aqueous layer was extracted with dichloromethane three times. The combined organic layer was washed with 1M aqueous NaOH, water, and brine, and dried over anhydrous Na_2SO_4. After removal of the solvent under reduced pressure, crude product was purified by column chromatography on silica gel twice (toluene/hexane = 2:1) to give (*S*)-3-(2,2′-dimethoxy-[1,1′-binaphthalen]-3-yl)perylene [(*S*)-**1**, 0.469 g, 72%] as yellow solid. The enantiomer (*R*)-**1** ($[\alpha]_D^{25}$ +166.7 (*c* 1.0, $CHCl_3$)) was synthesized using the same procedure as for the preparation of (*S*)-**1**.

(*S*)-3-(2,2′-Dimethoxy-[1,1′-binaphthalen]-3-yl)perylene [(*S*)-1]

Yellow solid; M.p. 248.0–248.9 ºC; $[\alpha]_D^{25}$ −160.7 (*c* 1.0, $CHCl_3$); IR (ATR): ν_{max} 3050, 2927, 1591, 1509, 1456, 1386, 1356, 1265, 1249, 1218, 1085, 1015, 825, 809 cm^{-1}; ^1H NMR (500 MHz, $CDCl_3$): δ (ppm) 8.28–8.26 (m, 1H), 8.22–8.17 (m, 3H), 8.00–7.97 (m, 2H), 7.92 (s, 0.47H), 7.90 (s, 0.53H), 7.88–7.85 (m, 1H), 7.76–7.70 (m, 1H), 7.68–7.65 (m, 3H), 7.49–7.40 (m, 5H), 7.37–7.22 (m, 5H), 3.89 (s, 1.6H), 3.82 (s, 1.4H), 3.03 (s, 1.4H), 2.98 (s, 1.6H); ^{13}C NMR (126 MHz, $CDCl_3$): δ(ppm) 155.0, 154.9, 154.8, 154.7, 136.9, 136.8, 134.7, 134.2, 134.1, 134.0, 133.8, 133.8, 133.6, 133.5, 131.5, 131.4, 131.3, 131.3, 131.2, 131.2, 131.1, 130.9, 130.9, 130.7, 130.7, 129.7, 129.6, 129.1, 129.0, 128.8, 128.6, 128.4, 128.2, 128.0, 127.8, 127.7, 126.8, 126.6, 126.6, 126.5, 126.5, 126.5, 126.3, 126.3, 125.7, 125.7, 125.4, 125.3, 125.2, 125.1, 125.0, 125.0, 123.6, 123.5, 120.3, 120.2, 119.8, 119.3, 119.2, 113.8, 113.4, 60.8, 60.7, 56.7, 56.5 (19 signals are hidden by incidental overlapping); HRMS-ESI (*m*/*z*): $[M]^+$ Calcd for $C_{42}H_{28}O_2$, 564.2084, Found, 564.2088.

3. NMR spectra and theoretical calculations

Calculation of bond rotation energy and exchange rate constants[3,4]

Exchange rate constant (k_c) at coalescence temperature (T_c = 413 K) is given by (1):

$$k_c = \frac{\pi}{\sqrt{2}}\Delta\delta_a = \frac{\pi}{\sqrt{2}} \times 33 \text{ Hz} = 73 \text{ s}^{-1} \quad (1)$$

where $\Delta\delta_a$ defined as the difference of chemical shift in Hz between the NMR signals under investigation.

The free energy of activation for bond rotation $\Delta G_c^{\pm}$ at coalescence temperature (T_c = 413 K) can be calculated using the Eyring equation (2):

$$\Delta G_c^{\pm} = -RT_c ln\left(\frac{hk_c}{k_B T_c}\right) = 88 \text{ kJ mol}^{-1} \quad (2)$$

where R = 8.314 J K^{-1} mol^{-1}, h = 6.626 × 10^{-34} J s^{-1}, k_B = 1.380 × 10^{-23} J s^{-1}.

Eyring formula (3) gives exchange rate constant (k_{rt}) at room temperature (T_{rt} = 298 K).

$$k_{rt} = \frac{k_B T_{rt}}{h} exp\left(-\frac{\Delta G_c^{\pm}}{RT_{rt}}\right) = 2.8 \times 10^{-3} \text{ s}^{-1} \quad (3)$$

Half-life at room temperature (T_{rt} = 298 K) is given by (4):

$$\tau_{rt} = \frac{ln2}{k_{rt}} = 2.5 \times 10^2 \text{ s} \quad (4)$$

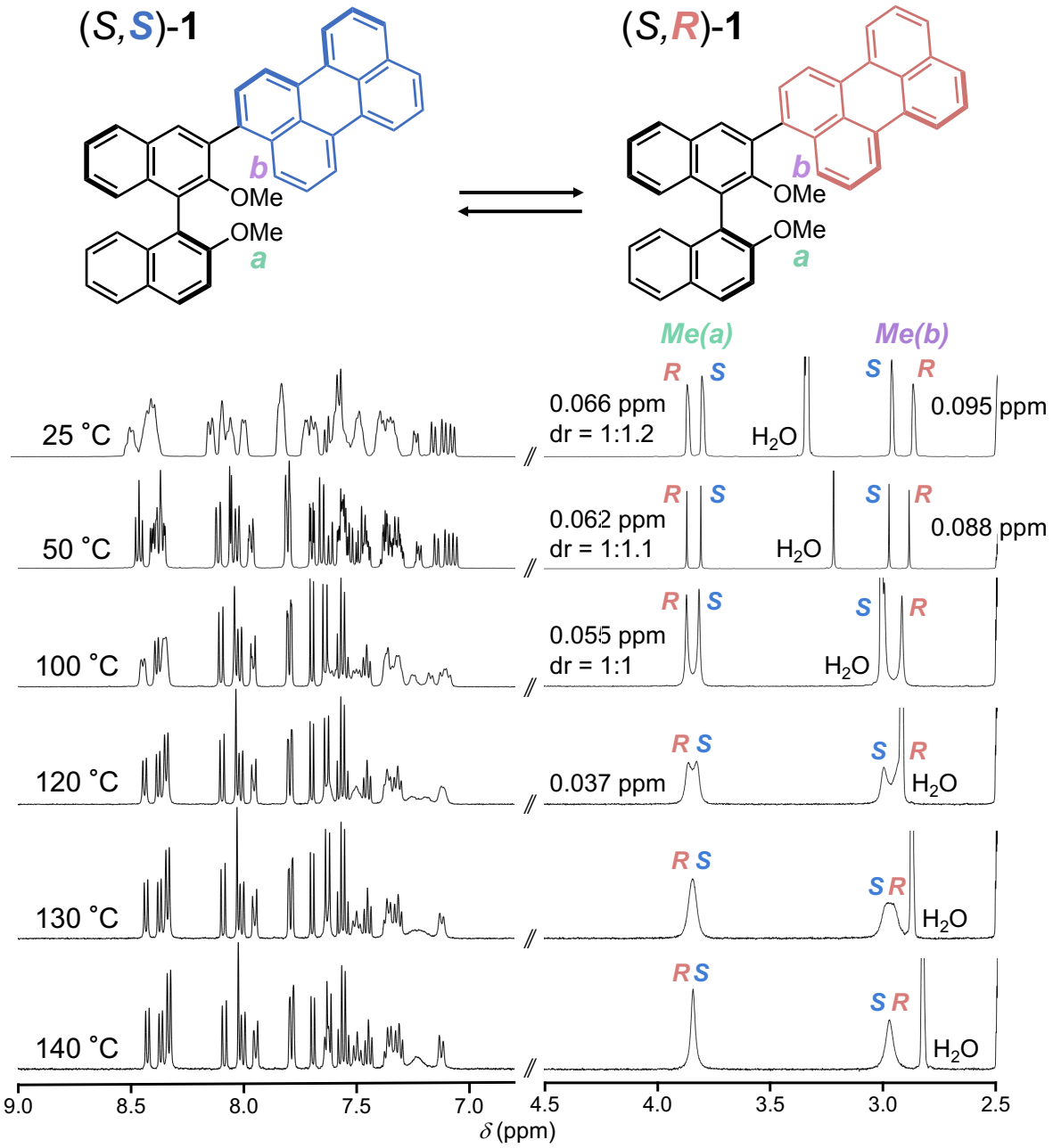

Fig. S1 Variable-temperature ^{1}H NMR spectra in the dynamic diastereomers (*S*,*S*)-**1** and (*S*,*R*)-**1** in DMSO-d_6.

*Theoretical calculations for NMR signals of (S,S)-**1** and (S,R)-**1** in $CDCl_3$*

The theoretical calculations were performed using the Gaussian 16 program.[5] Optimizations of the structures of (*S*,*S*)-**1** and (*S*,*R*)-**1** were carried out by density functional theory (DFT) calculations at the B3LYP/6-31G(d) level of theory, using the single-crystal X-ray diffraction structures of (*S*,*S*)-**1** and (*S*,*R*)-**1** in **Y**. Theoretical calculations for the ^{1}H and ^{13}C NMR signals of the optimized structures were performed at the B3LYP/6-311+G(2d,p) level.

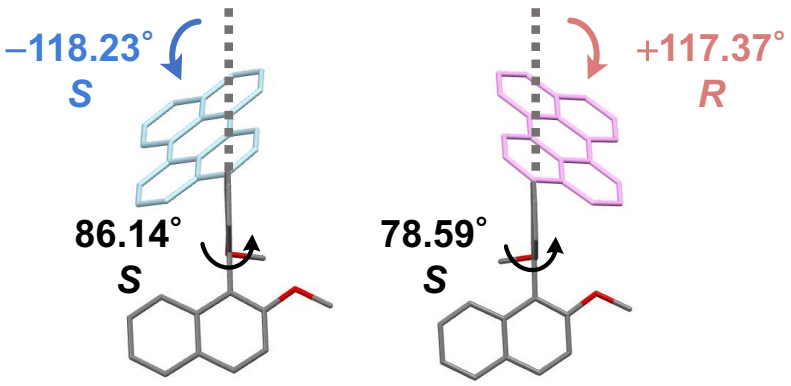

Fig. S2 Optimized structures of (*S*,*S*)-**1** and (*S*,*R*)-**1**.

Table S1. Simulated and experimental chemical shift values for the ^{1}H and ^{13}C NMR signals of Me(a) and Me(b) in (*S*,*S*)-**1** and (*S*,*R*)-**1**.

		^{1}H (ppm)		^{13}C (ppm)	
		Simulated	Experimental	Simulated	Experimental
(*S*,*S*)-**1**	Me(a)	3.38	3.82	45.43	56.46
	Me(b)	2.76	3.03	49.73	60.73
(*S*,*R*)-**1**	Me(a)	3.57	3.89	45.70	56.70
	Me(b)	2.49	2.98	50.06	60.81

4. Single-crystal X-ray diffraction analyses

The crystalline samples were mounted on a microloop. All measurements were made on a Rigaku XtaLAB P200 diffractometer using multi-layer mirror monochromated Cu-Kα radiation (λ = 1.54184 Å). The data were collected at a temperature of –150 ± 1 °C. The crystal-to-detector distance was 40.00 mm. Readout was performed in the 0.172 mm pixel mode. Data were collected and processed using CrysAlisPro (Rigaku Oxford Diffraction).[6] The data were corrected for Lorentz and polarization effects. Using Olex2,[7] the crystal structures of **G**, **YG**, and **Y** were solved with the SHELXT[8] structure solution program using Intrinsic Phasing. The refinement was carried out with the SHELXL[9] refinement package using least squares minimization. The non-hydrogen atoms were refined anisotropically. Hydrogen atoms were refined using the riding model.

*X-ray analysis of **G***

A single crystal of **G** was obtained from vapor diffusion of MeOH to a 1,4-dioxane solution of (*S*)-**1** (Fig. S3).

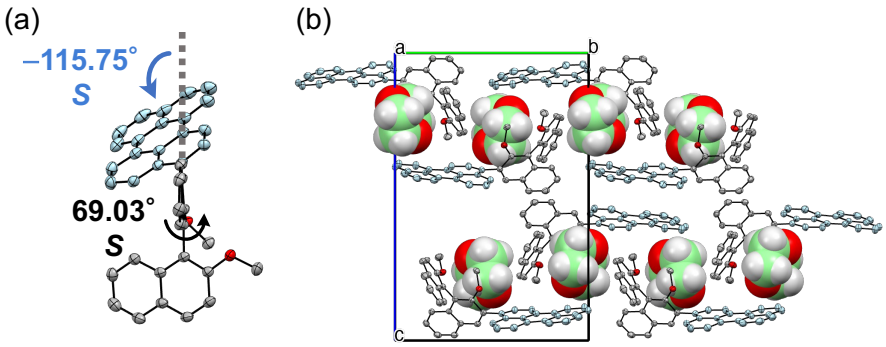

Fig. S3 (a) The molecular structure of (*S*,*S*)-**1** in **G**. (b) Packing structure of (*S*,*S*)-**1**•1,4-dioxane in **G** viewed along the *a*-axis. Atomic displacement parameters set at 50% probability, and all hydrogen atoms are omitted for clarity, except those in 1,4-dioxane molecules, which are depicted in the CPK model [Color code: C = dark gray, light blue (perylene), or light green (1,4-dioxane), O = red, H = light gray].

*X-ray analysis of **YG***

A single crystal of **YG** was obtained from vapor diffusion of MeOH to a toluene solution of (*S*)-**1** (Fig. S4).

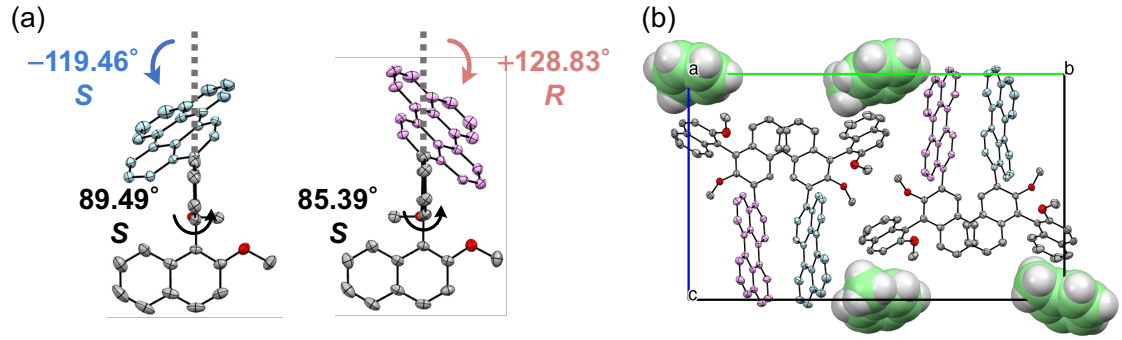

Fig. S4 (a) The molecular structures of (*S*,*S*)-**1** and (*S*,*R*)-**1** in **YG**. (b) Packing structure of (*S*,*S*)-**1**•(*S*,*R*)-**1**•toluene in **YG** viewed along the *a*-axis. Atomic displacement parameters set at 50% probability, and all hydrogen atoms are omitted for clarity, except those in toluene molecules, which are depicted in the CPK model [Color code: C = dark gray, light blue or light pink (perylene), or light green (toluene), O = red, H = light gray].

X-ray analysis of ***Y***

A single crystal of **Y** was obtained from vapor diffusion of MeOH to an ethyl acetate solution of (*S*)-**1** (Fig. S5).

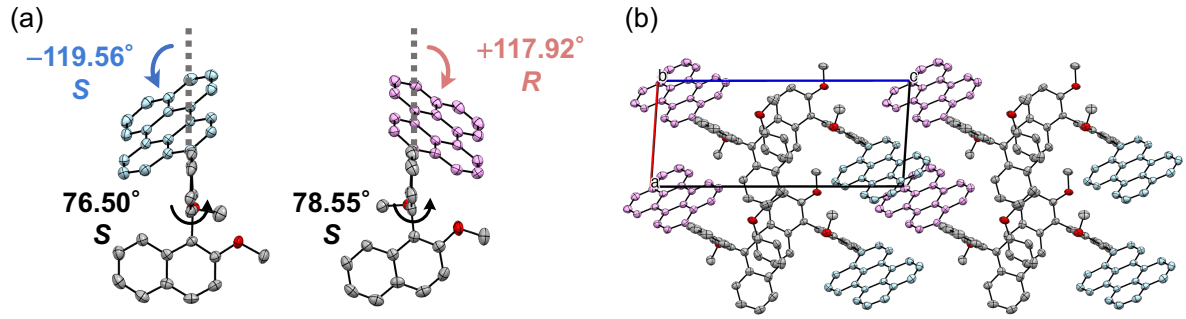

Fig. S5 (a) The molecular structures of (*S*,*S*)-**1** and (*S*,*R*)-**1** in **Y**. (b) Packing structure of (*S*,*S*)-**1**•(*S*,*R*)-**1** in **Y** viewed along the *b*-axis. Atomic displacement parameters set at 50% probability, and all hydrogen atoms are omitted for clarity [Color code: C = dark gray, light blue or light pink (perylene), O = red, H = light gray].

Table S2. Selected crystallographic data of **G**, **YG**, and **Y**.

	G (*S*,*S*)-**1**•**1,4-Dioxane**	**YG** (*S*,*S*)-**1**•(*S*,*R*)-**1**•**Toluene**	**Y** (*S*,*S*)-**1**•(*S*,*R*)-**1**
CCDC	2422979	2422980	2422981
Empirical formula	$C_{42}H_{28}O_2$•$C_4H_8O_2$	2($C_{42}H_{28}O_2$)•C_7H_8	$C_{42}H_{28}O_2$
Formula weight	652.75	1221.42	564.64
Temperature / K	123(2)	123(2)	123(2)
Crystal system	orthorhombic	monoclinic	triclinic
Space group	$P2_12_12_1$ (#19)	$P2_1$ (#4)	$P1$ (#1)
a / Å	9.62290(10)	7.66020(10)	7.8625(2)
b / Å	15.14060(10)	25.9534(3)	10.7582(4)
c / Å	22.4142(2)	15.6096(2)	18.3210(5)
α / °	90.0000	90.0000	76.600(3)
β / °	90.0000	95.2610(10)	89.561(2)
γ / °	90.0000	90.0000	72.009(3)
V / Å^3	3265.67(5)	3090.24(7)	1430.38(8)
Z	4	2	2
D_{calcd} / g cm^{-3}	1.328	1.313	1.311
μ / mm^{-1}	0.658	0.611	0.616
F(000)	1376	1284	592
Crystal size / mm^3	0.250 × 0.200 × 0.070	0.200 × 0.100 × 0.030	0.250 × 0.200 × 0.100
Radiation	CuKα (λ = 1.54184 Å)	CuKα (λ = 1.54184 Å)	CuKα (λ = 1.54184 Å)
2θ range for data collection / °	4.910 to 75.325	4.439 to 75.287	4.975 to 75.142
Index ranges	$-12 \le h \le 11$ $-18 \le k \le 13$ $-28 \le l \le 27$	$-9 \le h \le 9$ $-31 \le k \le 32$ $-19 \le l \le 18$	$-9 \le h \le 9$ $-13 \le k \le 13$ $-22 \le l \le 22$
Reflections collected	22792	38014	32394
Independent reflections	6550 [R_{int} = 0.0292]	12388 [R_{int} = 0.0392]	11019 [R_{int} = 0.0605]
Data / restraints / parameters	6550/0/454	12388/11/824	11019/3/798
Goodness-of-fit on F^2	1.049	1.060	1.029
Final R indexes [$I > 2\sigma(I)$]	R_1 = 0.0360, wR_2 = 0.0945	R_1 = 0.0521, wR_2 = 0.1395	R_1 = 0.0535, wR_2 = 0.1420
Final R indexes [all data]	R_1 = 0.0381, wR_2 = 0.0966	R_1 = 0.0570, wR_2 = 0.1441	R_1 = 0.0701, wR_2 = 0.1530
Largest diff. peak/hole / eÅ^{-3}	0.353/–0.219	0.753/–0.432	0.204/–0.198

5. Fluorescence spectra and PXRD patterns

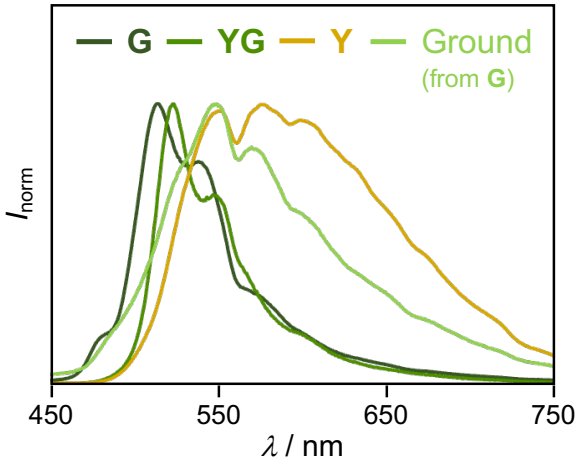

Fig. S6 Fluorescence spectra of crystal **G**, **YG**, **Y**, and ground from **G** (λ_{ex} = 367 nm).

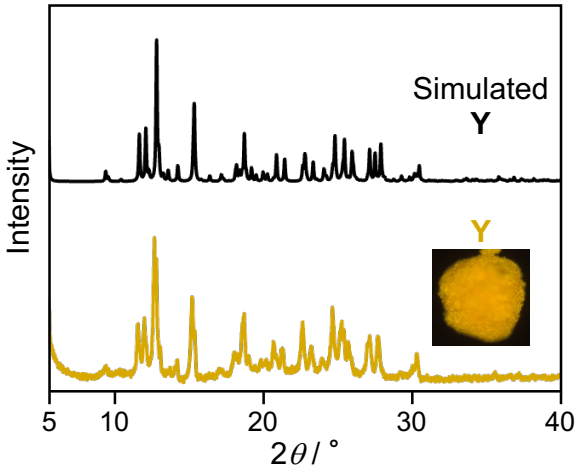

Fig. S7 Simulated PXRD pattern of **Y** obtained from ethyl acetate–methanol (black line) and experimental PXRD pattern of **Y** obtained from hot toluene–methanol (yellow line).

6. Absorption and CD spectra

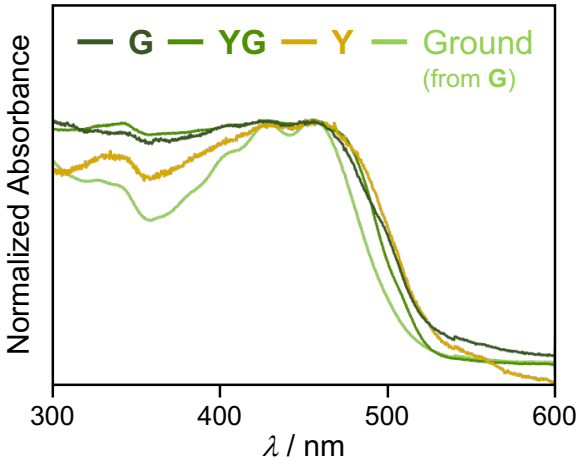

Fig. S8 Absorption spectra of crystal **G**, **YG**, **Y**, and ground from **G**.

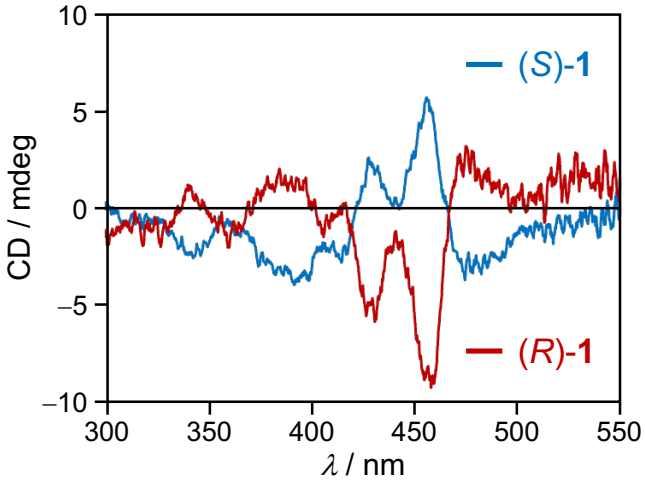

Fig. S9 CD spectra of crystal **G**.

7. Photophysical properties in solution

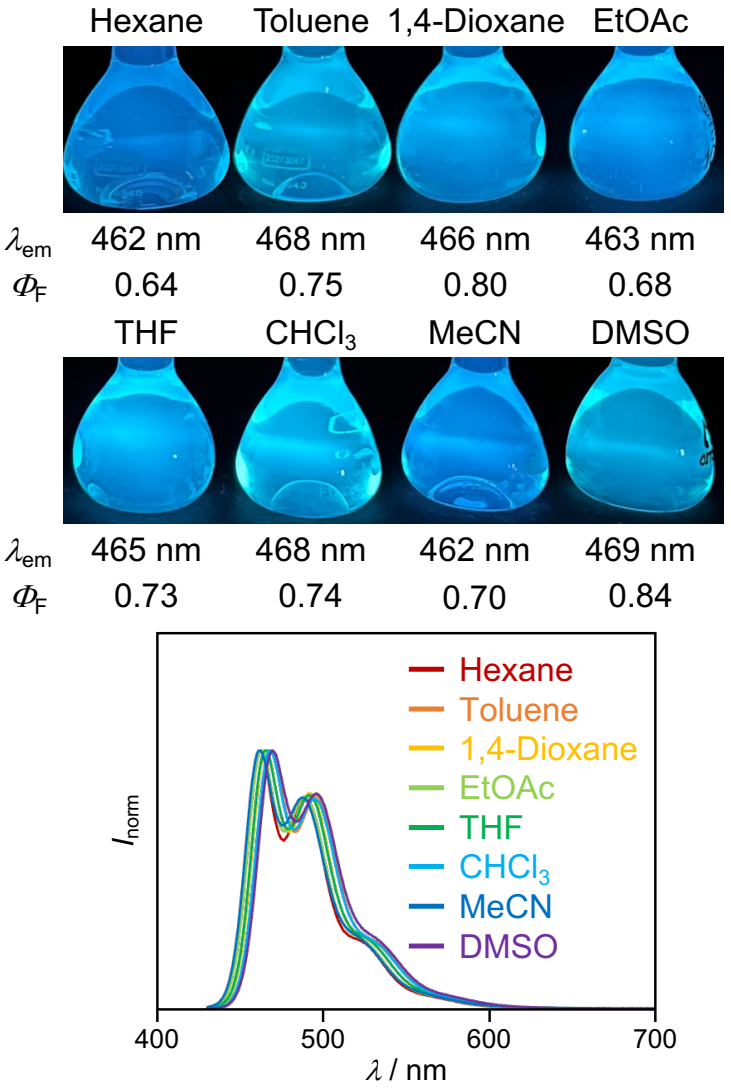

Fig. S10 Photographic images and fluorescence spectra (λ_{ex} = 420 nm) in various solvents (1.0×10^{-5} M).

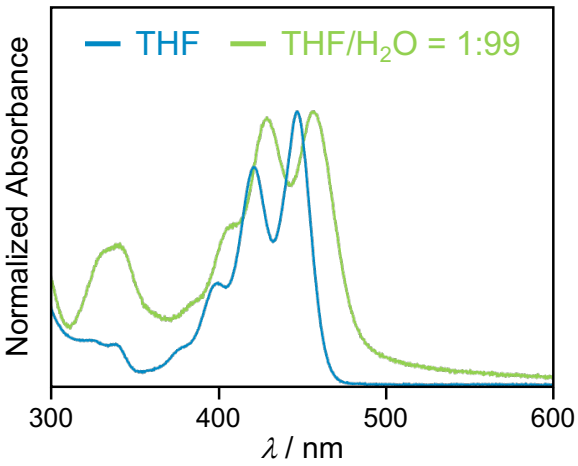

Fig. S11 Absorption spectra in THF and THF/H_2O = 1:99 (1.0×10^{-5} M).

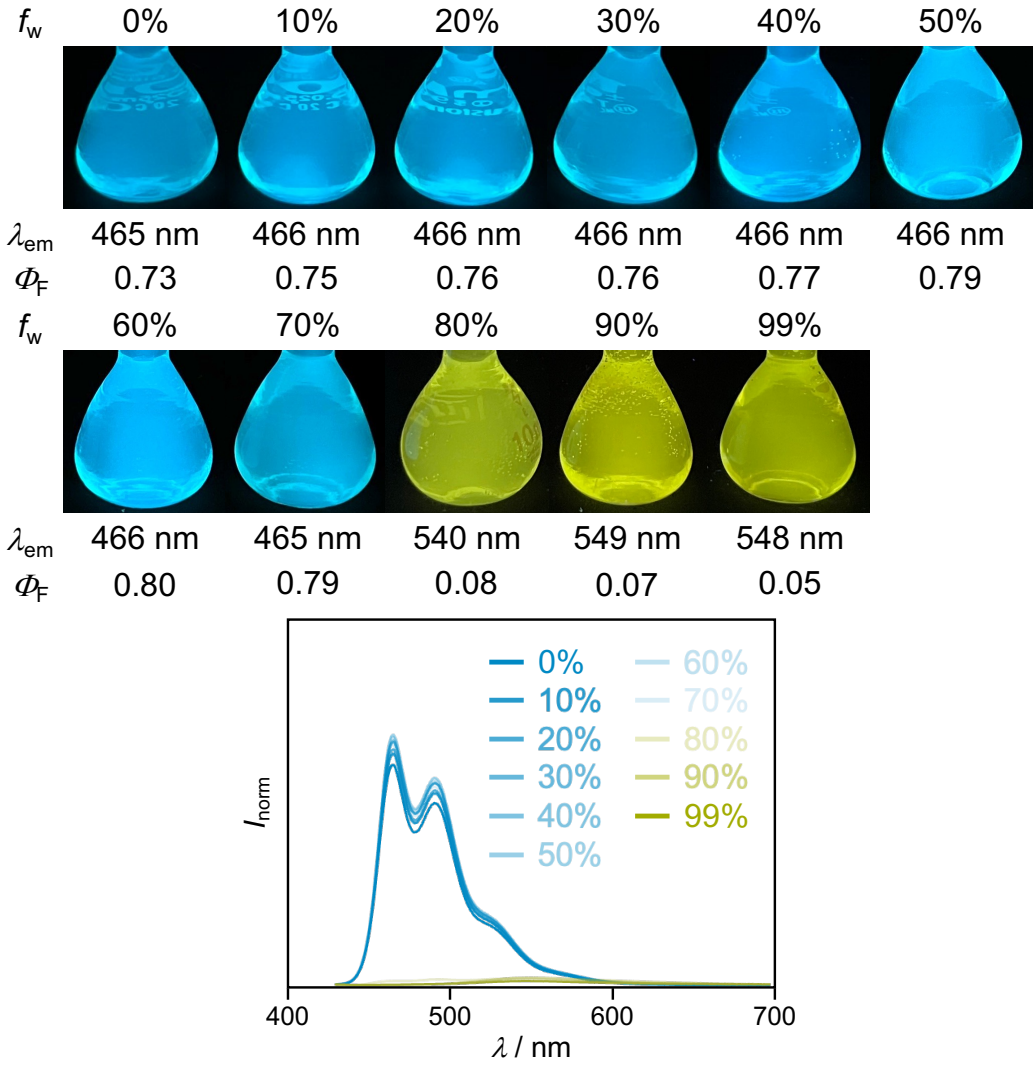

Fig. S12 Photographic images and fluorescence spectra (λ_{ex} = 420 nm) in THF/H_2O (1.0×10^{-5} M) with different water fractions (f_w vol%).

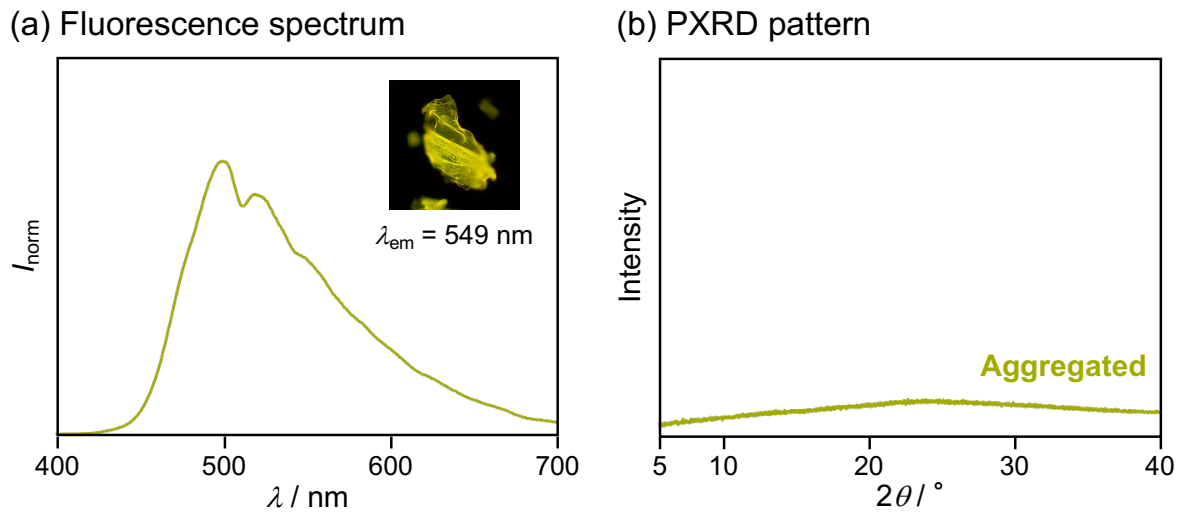

Fig. S13 (a) Photographic image and fluorescence spectrum (λ_{ex} = 367 nm) and (b) PXRD pattern of the aggregated amorphous sample formed in a THF/H_2O (1:99) mixed solvent and collected by filtration.

8. Fluorescence lifetime

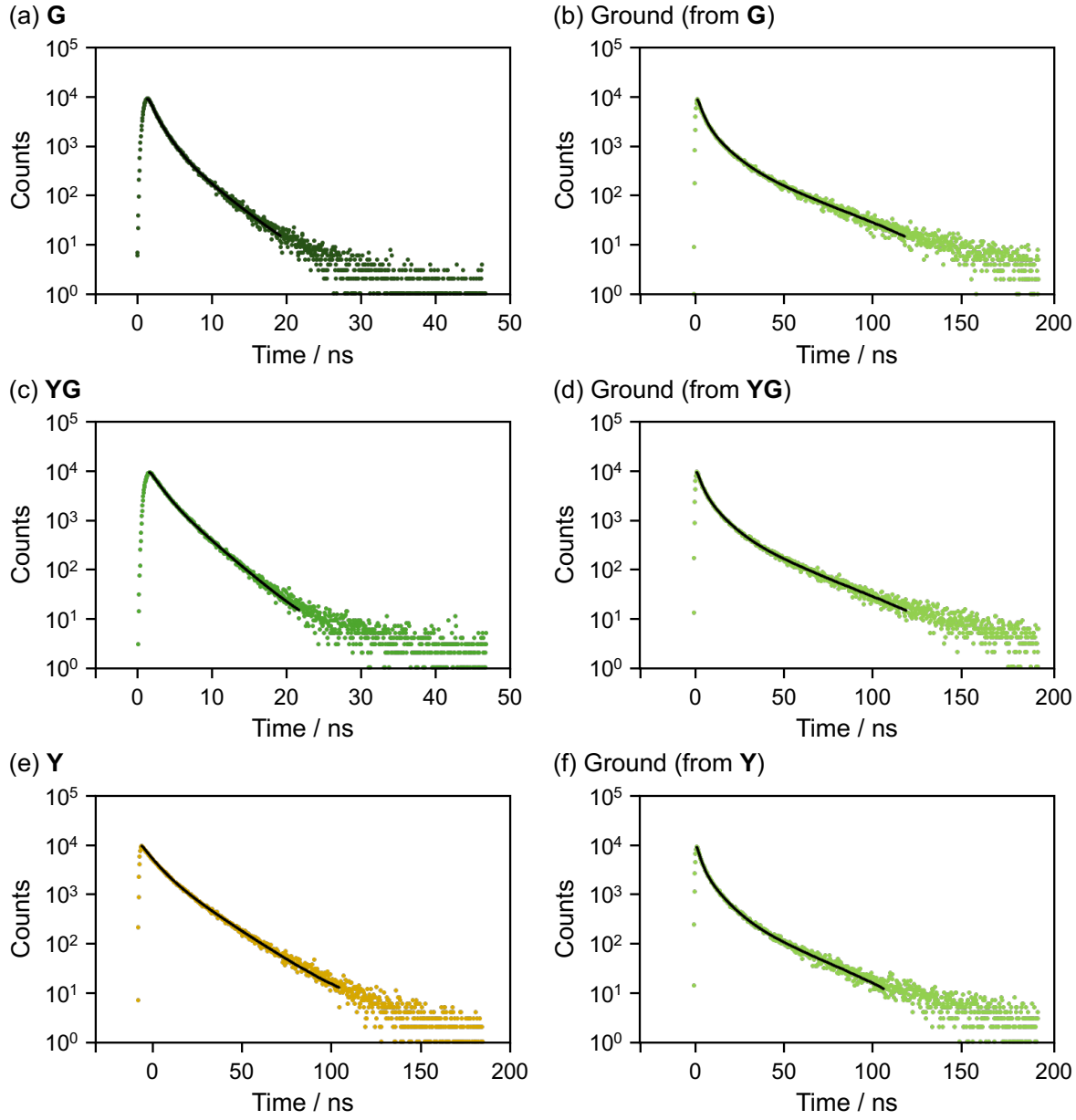

Fig. S14 Fluorescence decay profiles of crystal **G**, **YG**, **Y**, and their ground states (λ_{ex} = 405 nm).

Table S3 Fluorescence lifetime of crystal **G**, **YG**, **Y**, and their ground states (λ_{ex} = 405 nm).

Sample	λ_{obs} (nm)	τ_1 (ns)[a]	τ_2 (ns)[a]	τ_3 (ns)[a]	$\langle\tau\rangle$ (ns)[b]	χ^2	Φ_F	k_r ($\times10^8$ s^{-1})[c]	k_{nr} ($\times10^8$ s^{-1})[c]
G	515	0.35 (0.16)	1.4 (0.55)	3.6 (0.29)	1.9	0.9	0.21	1.2	4.2
YG	525	0.09 (0.02)	1.4 (0.40)	3.4 (0.58)	2.5	1.2	0.18	0.73	3.3
Y	575	0.17 (–0.02)	6.8 (0.43)	17.6 (0.59)	13.3	1.1	0.07	0.05	0.70
Ground (from G)	550	2.7 (0.29)	9.0 (0.43)	30.7 (0.28)	13.3	1.3	0.26	0.20	0.56
Ground (from YG)	550	2.5 (0.24)	8.2 (0.46)	27.7 (0.30)	12.7	1.2	0.25	0.20	0.59
Ground (from Y)	550	2.2 (0.29)	7.9 (0.47)	27.4 (0.24)	11.0	1.3	0.16	0.14	0.77

[a] The fractional contribution f_n of the component is indicated in parentheses.
[b] Intensity-weighted mean fluorescence lifetime. $\langle\tau\rangle = f_1\tau_1 + f_2\tau_2 + f_3\tau_3$
[c] Radiative rate constant (k_r) and non-radiative rate constant (k_{nr}) were calculated from $\Phi_F = k_r/(k_r + k_{nr}) = \langle\tau\rangle k_r$.

9. Stimuli-responsive luminescence

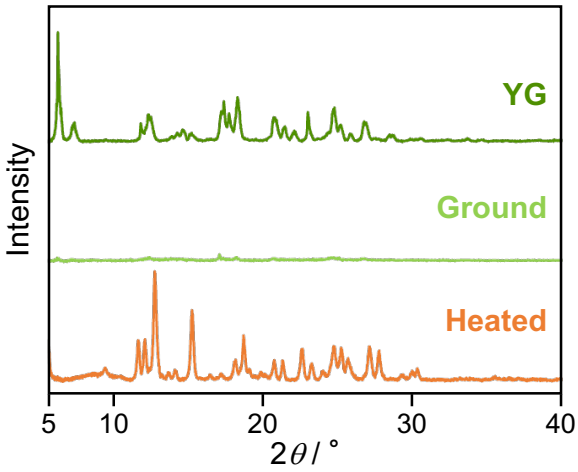

Fig. S15 PXRD patterns of crystal **YG**, after grinding **YG**, and after heating ground **YG**.

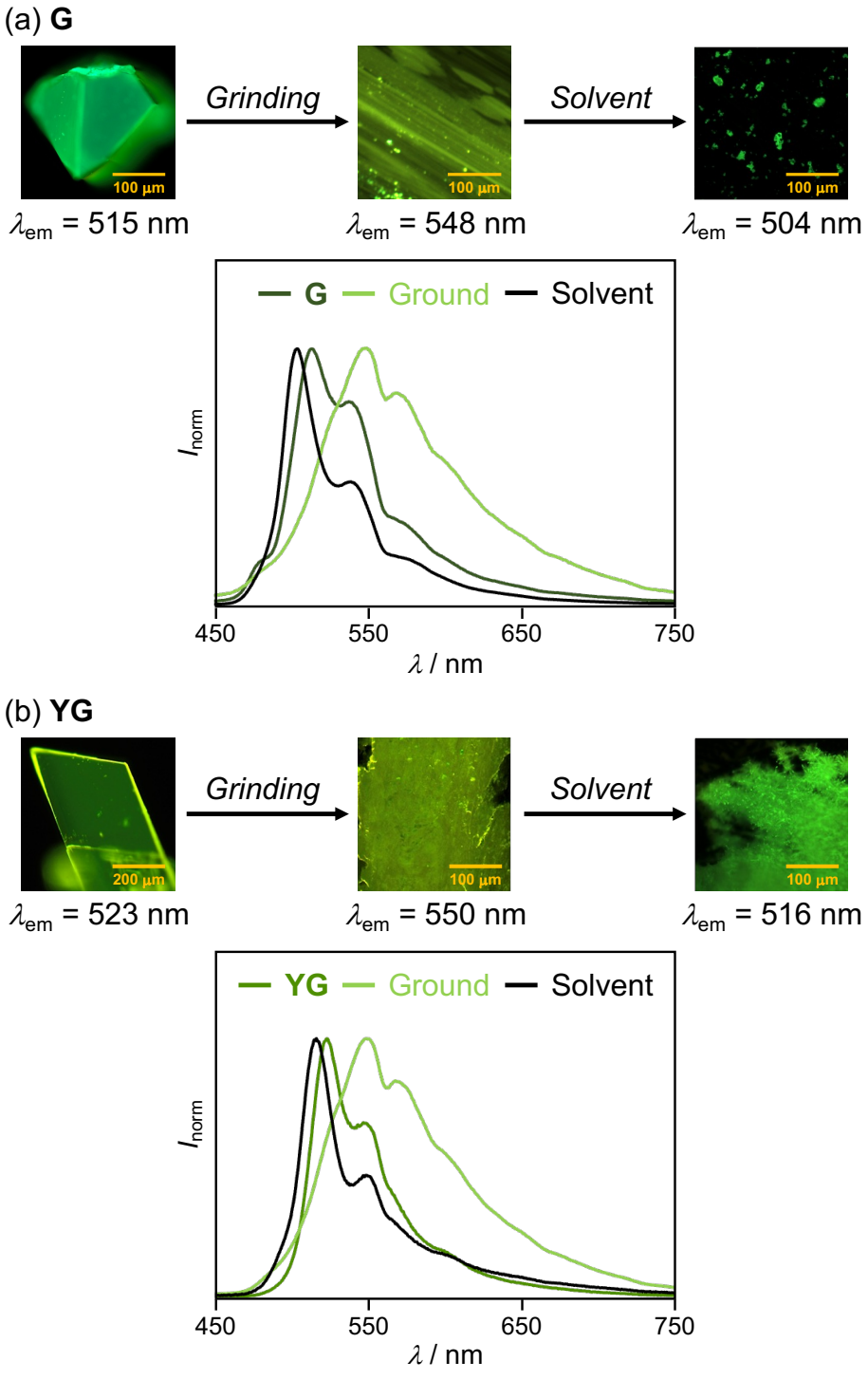

Fig. S16 Photographic images and fluorescence spectra (λ_{ex} = 367 nm) of (a) crystal **G**, after grinding, and after treated with 1,4-dioxane and (b) crystal **YG**, after grinding, and after treated with toluene.

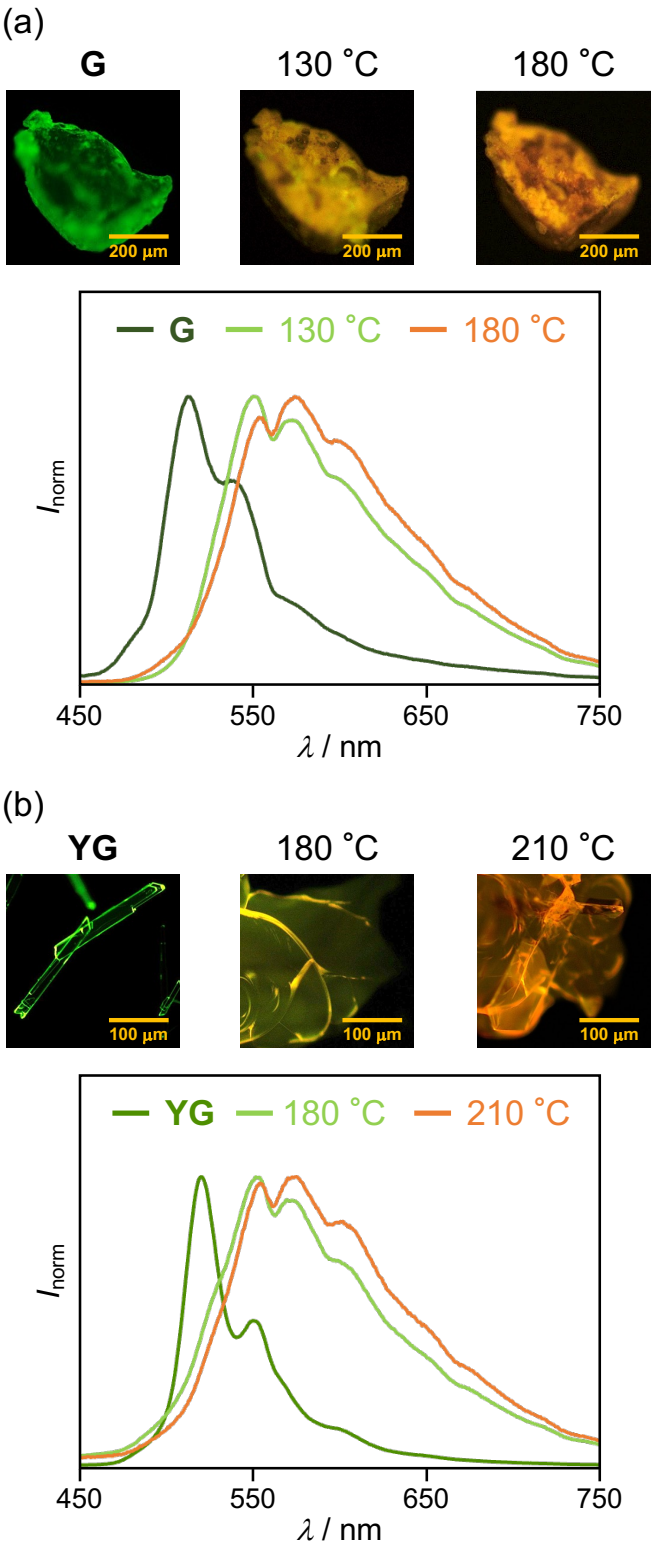

Fig. S17 Photographic images and fluorescence spectra (λ_{ex} = 367 nm) for thermoresponsive luminescence of (a) **G** and (b) **YG**.

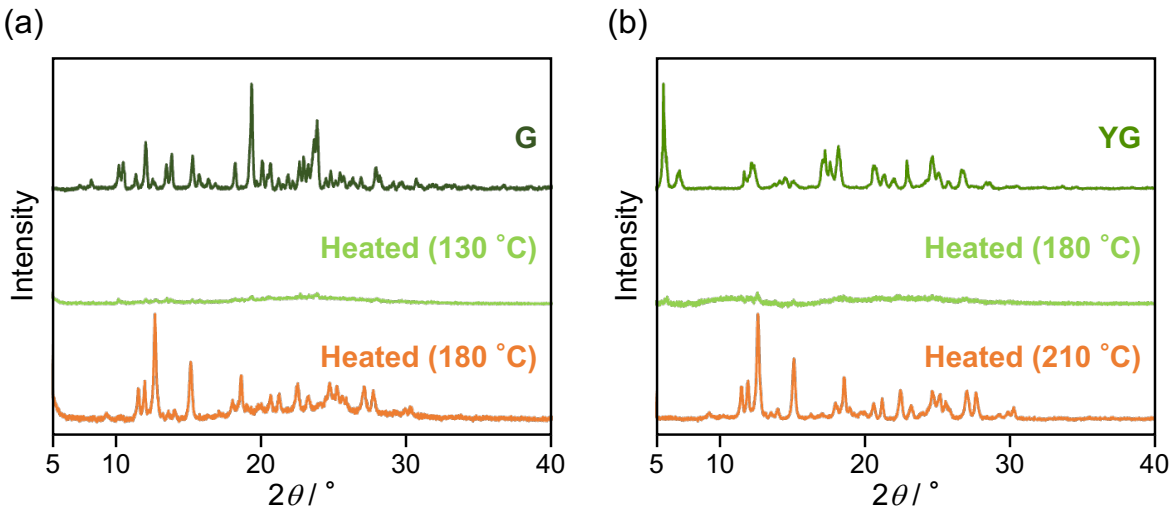

Fig. S18 PXRD patterns of heated samples of (a) crystal **G** and (b) **YG**.

10. Cartesian coordinates for optimized structures of (*S*,*S*)-1 and (*S*,*R*)-1

*Coordinates of (S,S)-**1** in the ground state*

B3LYP/6-31G(d) level

Sum of electronic and zero-point energies (au) = –1767.258671

Number of imaginary frequency: 0

Center Number	Atomic Number	Atomic Type	Coordinates (Angstroms) X	Y	Z
1	8	0	1.090023	0.561222	0.969177
2	8	0	4.075020	-1.276628	2.279417
3	6	0	2.889176	-0.574201	-0.095652
4	6	0	1.528318	-0.440239	0.130179
5	6	0	0.566305	-1.278569	-0.519838
6	6	0	1.028656	-2.262935	-1.371648
7	1	0	0.311567	-2.904399	-1.878245
8	6	0	2.409561	-2.446570	-1.632233
9	6	0	2.870960	-3.454694	-2.520994
10	1	0	2.138387	-4.100387	-2.999950
11	6	0	4.214224	-3.612893	-2.774071
12	1	0	4.555483	-4.387199	-3.455861
13	6	0	5.155043	-2.761576	-2.146735
14	1	0	6.214749	-2.888114	-2.352366
15	6	0	4.739225	-1.774024	-1.281068
16	1	0	5.466053	-1.123037	-0.806474
17	6	0	3.359511	-1.585181	-0.995119
18	6	0	3.853490	0.340269	0.594384
19	6	0	4.448688	-0.052324	1.789304
20	6	0	5.376502	0.787899	2.455730
21	1	0	5.830707	0.471049	3.387356
22	6	0	5.700129	2.014318	1.923507
23	1	0	6.410626	2.656263	2.438917
24	6	0	5.125158	2.462694	0.710173
25	6	0	5.454792	3.725537	0.147564

26	1	0	6.164316	4.359204	0.675210
27	6	0	4.893618	4.140462	-1.037042
28	1	0	5.152809	5.107778	-1.458582
29	6	0	3.974427	3.299661	-1.711606
30	1	0	3.535844	3.628853	-2.650040
31	6	0	3.631694	2.072201	-1.192584
32	1	0	2.930348	1.435021	-1.720917
33	6	0	4.188951	1.610715	0.034196
34	6	0	0.764165	0.143222	2.297825
35	1	0	0.497910	1.051150	2.843546
36	1	0	-0.089306	-0.545406	2.300996
37	1	0	1.624746	-0.339573	2.774602
38	6	0	4.739777	-1.791432	3.422090
39	1	0	4.323743	-2.788053	3.581476
40	1	0	5.822239	-1.873944	3.258739
41	1	0	4.555049	-1.178509	4.314383
42	6	0	-0.899830	-1.149783	-0.272468
43	6	0	-1.579972	-2.235023	0.253040
44	1	0	-1.026923	-3.137197	0.499745
45	6	0	-2.960135	-2.192505	0.497589
46	1	0	-3.423560	-3.077836	0.917648
47	6	0	-3.720242	-1.061700	0.225160
48	6	0	-5.168895	-1.008830	0.500594
49	6	0	-5.854630	-2.076996	1.072012
50	1	0	-5.327060	-2.986569	1.335402
51	6	0	-7.235981	-2.022028	1.330240
52	1	0	-7.728190	-2.881774	1.776796
53	6	0	-7.955350	-0.890640	1.021921
54	1	0	-9.023291	-0.838160	1.218286
55	6	0	-7.310230	0.231027	0.442315
56	6	0	-8.039592	1.404476	0.124368
57	1	0	-9.106566	1.431790	0.330721
58	6	0	-7.400185	2.486880	-0.433861
59	1	0	-7.955986	3.388553	-0.676626

60	6	0	-6.019040	2.439093	-0.695676
61	1	0	-5.558064	3.317316	-1.132685
62	6	0	-5.251947	1.313595	-0.408555
63	6	0	-3.801446	1.258063	-0.683147
64	6	0	-3.126377	2.323037	-1.269053
65	1	0	-3.660246	3.226273	-1.541128
66	6	0	-1.749235	2.267153	-1.536389
67	1	0	-1.261293	3.118319	-2.003252
68	6	0	-1.020536	1.147178	-1.211451
69	1	0	0.041188	1.109272	-1.421623
70	6	0	-1.645930	0.029407	-0.602766
71	6	0	-3.061116	0.075667	-0.346603
72	6	0	-5.900975	0.178350	0.175563

---

*Coordinates of (S,R)-**1** in the ground state*

B3LYP/6-31G(d) level

Sum of electronic and zero-point energies (au) = –1767.258987

Number of imaginary frequency: 0

Center Number	Atomic Number	Atomic Type	Coordinates (Angstroms) X	Y	Z
1	8	0	1.068877	-0.839877	0.657471
2	8	0	3.000746	-2.004070	-1.693508
3	6	0	2.858746	0.366932	-0.349692
4	6	0	1.512612	0.265729	-0.036083
5	6	0	0.559786	1.244028	-0.462309
6	6	0	1.017884	2.336357	-1.173079
7	1	0	0.306157	3.086488	-1.509334
8	6	0	2.384790	2.493300	-1.512628
9	6	0	2.841247	3.612097	-2.260480
10	1	0	2.118010	4.367663	-2.558840
11	6	0	4.167313	3.738605	-2.605108

12	1	0	4.504687	4.598583	-3.177340
13	6	0	5.094962	2.742389	-2.217085
14	1	0	6.140428	2.843824	-2.496179
15	6	0	4.684273	1.645953	-1.491423
16	1	0	5.401395	0.885984	-1.199660
17	6	0	3.322826	1.487479	-1.112338
18	6	0	3.798449	-0.710571	0.090726
19	6	0	3.834796	-1.910399	-0.616236
20	6	0	4.705761	-2.959089	-0.226289
21	1	0	4.725816	-3.888609	-0.783028
22	6	0	5.531028	-2.802413	0.863250
23	1	0	6.196776	-3.610547	1.156932
24	6	0	5.533346	-1.604291	1.616428
25	6	0	6.378263	-1.431109	2.746112
26	1	0	7.039920	-2.247246	3.028131
27	6	0	6.362888	-0.262463	3.470454
28	1	0	7.013076	-0.141463	4.332478
29	6	0	5.492524	0.788355	3.089012
30	1	0	5.482228	1.711292	3.663042
31	6	0	4.661962	0.654689	1.999665
32	1	0	4.003429	1.469007	1.716075
33	6	0	4.651118	-0.541725	1.223577
34	6	0	0.893669	-0.646997	2.062884
35	1	0	0.523804	-1.596569	2.455990
36	1	0	1.846105	-0.397132	2.546245
37	1	0	0.159224	0.140881	2.269476
38	6	0	2.968200	-3.211840	-2.435790
39	1	0	2.233239	-3.052220	-3.226920
40	1	0	3.941656	-3.436899	-2.891429
41	1	0	2.652550	-4.061194	-1.816058
42	6	0	-0.892605	1.126474	-0.142938
43	6	0	-1.493999	2.121786	0.607313
44	1	0	-0.889769	2.947163	0.974036
45	6	0	-2.859499	2.081680	0.924878

46	1	0	-3.260659	2.892043	1.522704
47	6	0	-3.682141	1.045165	0.501366
48	6	0	-5.113976	0.990231	0.853711
49	6	0	-5.715999	1.949987	1.662489
50	1	0	-5.131540	2.769299	2.065186
51	6	0	-7.082812	1.896742	1.989326
52	1	0	-7.508506	2.669756	2.623420
53	6	0	-7.871558	0.875818	1.511687
54	1	0	-8.929203	0.826258	1.758135
55	6	0	-7.312588	-0.134517	0.688858
56	6	0	-8.113762	-1.194521	0.194357
57	1	0	-9.168957	-1.220773	0.454425
58	6	0	-7.557503	-2.170309	-0.599661
59	1	0	-8.168821	-2.984445	-0.979615
60	6	0	-6.190325	-2.126203	-0.927133
61	1	0	-5.795917	-2.918662	-1.552628
62	6	0	-5.354887	-1.109871	-0.472477
63	6	0	-3.917585	-1.061235	-0.810435
64	6	0	-3.321678	-2.026271	-1.614592
65	1	0	-3.909482	-2.844830	-2.013866
66	6	0	-1.957471	-1.974447	-1.942304
67	1	0	-1.533722	-2.745359	-2.580327
68	6	0	-1.160986	-0.960172	-1.464433
69	1	0	-0.108652	-0.928011	-1.719989
70	6	0	-1.705900	0.051607	-0.632527
71	6	0	-3.106631	0.010220	-0.306838
72	6	0	-5.917914	-0.084301	0.353657

---

11. References

1) F. Yang, S. Wei, C.-A. Chen, P. Xi, L. Yang, J. Lan, H.-M. Gau and J. You, *Chem. –Eur. J.,* 2008, **14**, 2223.

2) A. R. Karikachery, H. B. Lee, M. Masjedi, A. Ross, M. A. Moody, X. Cai, M. Chui, C. D. Hoff and P. R. Sharp, *Inorg. Chem.,* 2013, **52**, 4113.

3) W. E. Stewart and T. H. Siddall, *Chem. Rev.*, 1970, **70**, 517.

4) P. A. Otten, S. Gorter and A. van der Gen, *Chem. Ber.*, 1997, **130**, 49.

5) Gaussian 16, Revision A.03, M. J. Frisch, G. W. Trucks, H. B. Schlegel, G. E. Scuseria, M. A. Robb, J. R. Cheeseman, G. Scalmani, V. Barone, G. A. Petersson, H. Nakatsuji, X. Li, M. Caricato, A. V. Marenich, J. Bloino, B. G. Janesko, R. Gomperts, B. Mennucci, H. P. Hratchian, J. V. Ortiz, A. F. Izmaylov, J. L. Sonnenberg, D. Williams-Young, F. Ding, F. Lipparini, F. Egidi, J. Goings, B. Peng, A. Petrone, T. Henderson, D. Ranasinghe, V. G. Zakrzewski, J. Gao, N. Rega, G. Zheng, W. Liang, M. Hada, M. Ehara, K. Toyota, R. Fukuda, J. Hasegawa, M. Ishida, T. Nakajima, Y. Honda, O. Kitao, H. Nakai, T. Vreven, K. Throssell, J. A. Montgomery, Jr., J. E. Peralta, F. Ogliaro, M. J. Bearpark, J. J. Heyd, E. N. Brothers, K. N. Kudin, V. N. Staroverov, T. A. Keith, R. Kobayashi, J. Normand, K. Raghavachari, A. P. Rendell, J. C. Burant, S. S. Iyengar, J. Tomasi, M. Cossi, J. M. Millam, M. Klene, C. Adamo, R. Cammi, J. W. Ochterski, R. L. Martin, K. Morokuma, O. Farkas, J. B. Foresman and D. J. Fox, Gaussian, Inc., Wallingford CT, 2016.

6) CrysAlisPro: Data Collection and Processing Software, Rigaku Corporation (2015). Tokyo 196-8666, Japan.

7) O. V. Dolomanov, L. J. Bourhis, R. J. Gildea, J. A. K. Howard and H. Puschmann, *J. Appl. Crystallogr.*, 2009, **42**, 339.

8) G. M. Sheldrick, *Acta Cryst.*, 2015, **A71**, 3.

9) G. M. Sheldrick, *Acta Cryst.*, 2015, **C71**, 3.

^{1}H NMR spectrum of (*S*)-**1** (500 MHz, $CDCl_3$, rt)

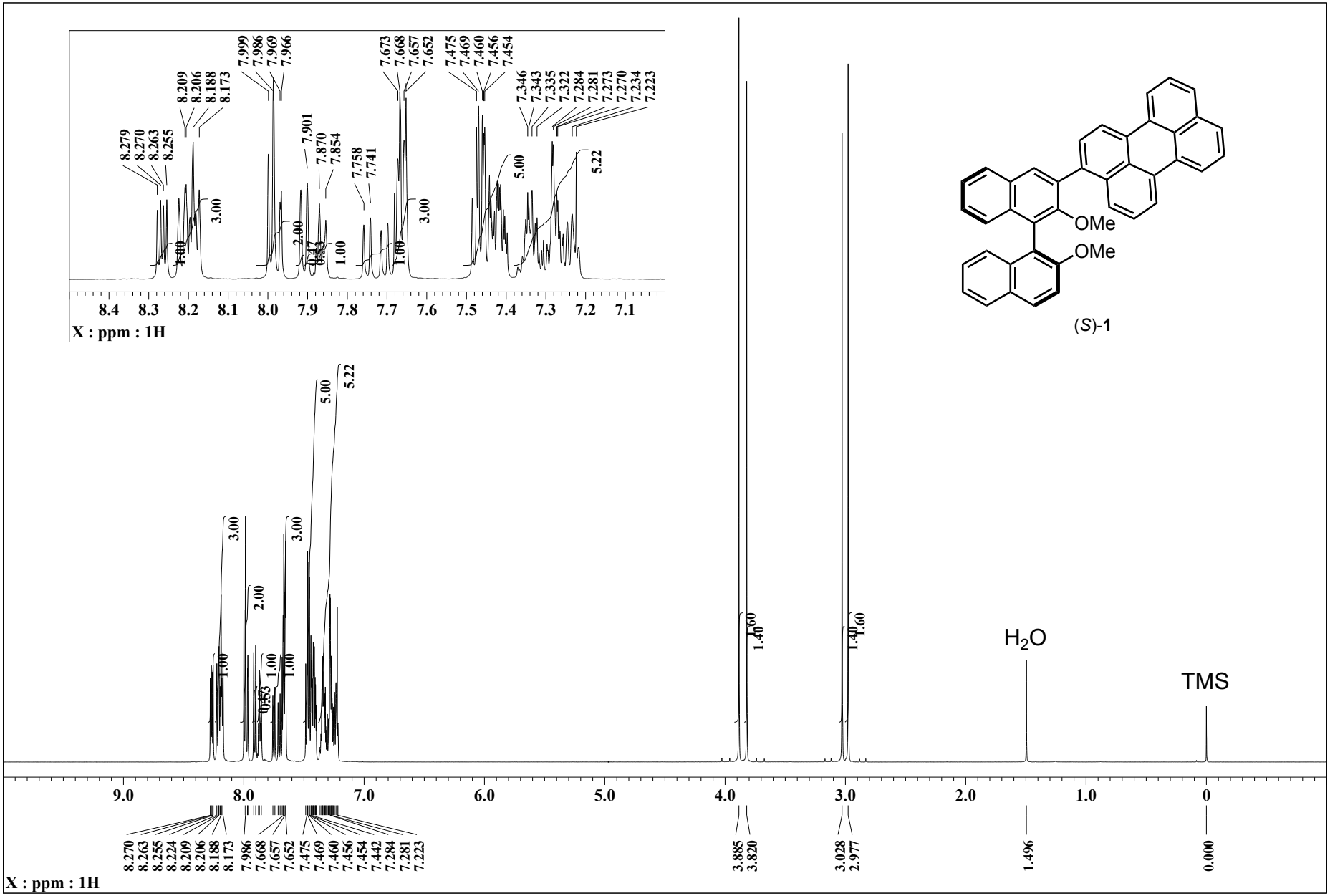

^{13}C NMR spectrum of (*S*)-**1** (126 MHz, $CDCl_3$, rt)